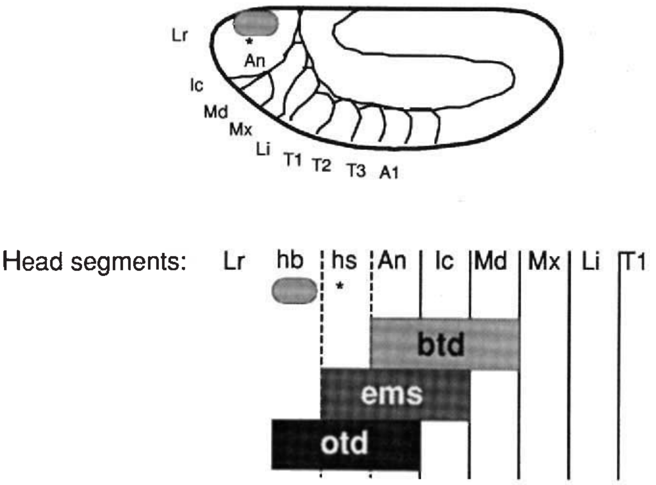

FIG. 3 Schematic representation of the segmental defects in the mutants. The *btd* gene is required for development of the mandibular, intercalary and antennal segments, but not for maxillary and pre-antennal regions. The *ems* gene is required in intercalary and antennal segments and in a part of the pre-antennal domain—defined by the *en* head spot (hs)—but not in more anterior pre-antennal regions—defined by the *wg* head blob (hb)—or in the mandibular segment. The *otd* gene is required in the antennal segment and both pre-antennal regions, but not in intercalary or mandibular segments. The domains in which the genes are required overlap and are out of phase by one segment at their posterior limits. The anterior limit of the domain of action of *btd*, *ems* and *otd* are also out of phase, occupying progressively greater portions of the pre-antennal region. Their effects on *en* and *wg* expression anteriorly may reflect cryptic segmentation in the pre-antennal region of the head. These domains (hs and hb) are indicated with dashed lines to point out that they may not be true segments. Jürgens *et al.*[30] and Struhl[31] both propose six head segments. None of the genes analysed here affects the labral segment (Lr).

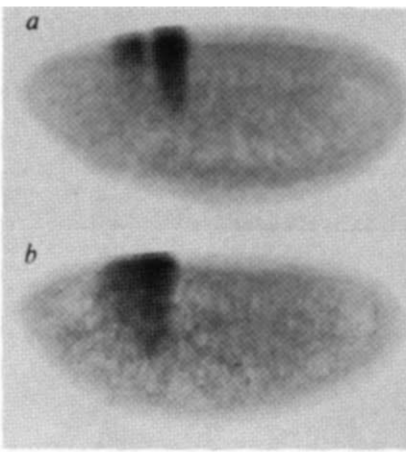

FIG. 4 The pattern of expression of *Dll* is altered at the blastoderm stage in *btd* mutant embryos. *Dll* is first expressed during cellularization of the blastoderm, in two bands that are restricted in their dorsal-ventral extents[20]. Double-labelling with probes that detect *Dll* and *wingless* shows that the more posterior band corresponds to the primordium of the maxillary and labial limbs (which resolves at a later stage into discrete primordia; data not shown). Following the development of the mature pattern of *Dll* expression suggests that the anterior band corresponds to the presumptive antennal primordium[20]. In *btd* mutant embryos only one broadened stripe of *Dll* expression is seen at the blastoderm stage. As the mandibular, intercalary and antennal segments are absent at later stages in *btd* mutant embryos, it seems likely that the broadened *Dll* band observed reflects a deletion of the early antennal primordium with a concomitant anterior expansion of the maxillary-labial stripe. In the absence of hybridization probes that distinguish these primordia at the blastoderm stage, this suggestion cannot be directly tested.

Received 3 April; accepted 25 May 1990.

1. Nüsslein-Volhard, C., Frohnhöfer, H. G. & Lehmann, R. *Science* **238**, 1675–1681 (1987).
2. Frohnhöfer, H. G. & Nüsslein-Volhard, C. *Nature* **324**, 120–125, G. (1986).
3. Frigerio, G., Burri, M., Bopp, D., Baumgartner, S. & Noll, M. *Cell* **47**, 735–746 (1986).
4. Berleth, T. *et al. EMBO J.* **7**, 1749–1756 (1988).
5. Driever, W. & Nüsslein-Volhard, C. *Cell* **54**, 83–93 (1988).
6. Driever, W. & Nüsslein-Volhard, C. *Cell* **54**, 95–104 (1988).
7. Driever, W. & Nüsslein-Volhard, C. *Nature.* **337**, 138–143 (1989).
8. Struhl, G., Struhl, K. & McDonald, P. *Cell.* **57**, 1259–1273 (1989).
9. Tautz, D. *et al. Nature* **327**, 383–389 (1987).
10. Tautz, D. *Nature* **332**, 281–284 (1988).
11. Schröder, C., Tautz, D., Seifert, E. & Jäckle *EMBO J.* **7**, 2881–2887 (1988).
12. Driever, W., Thoma, G. & Nüsslein-Volhard, C. *Nature* **340**, 363–367 (1989).
13. Lehmann, R. & Nüsslein-Volhard, C. *Devl Biol* **119**, 404–417 (1987).
14. Bender, M., Turner, F. R. & Kaufman, T. C. *Devl Biol* **119**, 418–432 (1987).
15. Wieschaus, E., Nüsslein-Volhard, C. & Jürgens, G. *Roux's Arch. dev. Biol.* **193**, 296–307 (1984).
16. Jürgens, G., Wieschaus, E. & Nüsslein-Volhard, C. *Roux's Arch. dev. Biol.* **193**, 283–295 (1984).
17. Dalton, D., Chadwick, R. & McGinnis, W. *Genes Dev.* **3**, 1940–1956 (1989).
18. Cohen, S. M. & Jürgens, G. *EMBO J.* **8**, 2045–2055 (1989).
19. Sunkel, C. E. & Whittle, J. R. S. *Roux's Arch. dev. Biol.* **196**, 124–132 (1987).
20. Cohen, S. M. *Nature* **343**, 173–177 (1990).
21. Baker, N. E. *Development* **103**, 289–298 (1988).
22. Mahaffey, J. W., Diederich, R. J. & Kaufman, T. C. *Development* **105**, 167–174 (1989).
23. Stanojevic, D., Hoey, T. & Levine, M. *Nature* **341**, 331–335 (1989).
24. Pankratz, M. J. *et al. Cell* **61**, 309–317 (1990).
25. Lawrence, P. A., Johnston, P., Macdonald, P. & Struhl, G. *Nature* **328**, 440–442 (1987).
26. Akam, M. *Development* **101**, 1–22 (1987).
27. Ingham, P. *Nature* **335**, 25–34 (1988).
28. Tautz, D. & Pfeifle, C. *Chromosoma* **98**, 81–85 (1989).
29. Lawrence, P. A. & Johnston, P. *Development* **105**, 761–767 (1989).
30. Jürgens, G., Lehmann, R., Schardin, M. & Nüsslein-Volhard, C. *Roux's Arch. dev. Biol.* **195**, 359–377 (1986).
31. Struhl, G. *Devl Biol.* **84**, 386–396 (1981).
32. Finkelstein, R. & Perrimon, N. *Nature*, **346**, 485–488 (1990).

ACKNOWLEDGEMENTS. We thank Herbert Jäckle for supporting this work in his lab through a grant from the DFG Leibniz program; Bill McGinnis for providing fly strains, antibody to *ems* and for stimulating discussion; Bob Finkelstein and Wolfgang Driever for communicating their unpublished results, which were of considerable importance to the work presented here; P. Ingham for the *wg* cDNA, and P. Lawrence for the *en* antibody.

The *orthodenticle* gene is regulated by *bicoid* and *torso* and specifies *Drosophila* head development

Robert Finkelstein & Norbert Perrimon

Department of Genetics and Howard Hughes Medical Institute, Harvard Medical School, 25 Shattuck Street, Boston, Massachusetts 02115, USA

IN the *Drosophila* embryo, cell fate along the anterior–posterior axis is determined by maternally expressed genes[1,2]. The activity of the *bicoid* (*bcd*) gene is required for the development of larval head and thoracic structures[3], and that of maternal *torso* (*tor*)[1] for the development of the unsegmented region of the head (acron). In contrast to the case of thoracic and abdominal segmentation[4,5], the hierarchy of zygotically expressed genes controlling head development has not been clearly defined. The *bcd* protein, which is expressed in a gradient[6], activates zygotic expression of the gap gene *hunchback* (*hb*)[7,8], but *hb* alone is not sufficient to specify head development. Driever *et al.*[9] proposed that at least one other *bcd*-activated gene controls the development of head regions anterior to the *hb* domain. We report here that the homeobox gene *orthodenticle* (*otd*), which is involved in head development, could be such a gene. We also show that *otd* expression responds to the activity of the maternal *tor* gene at the anterior pole of the embryo.

Mutations at the *otd* locus cause embryonic lethality, head involution fails to occur properly and several larval cuticular and sensory head structures are deleted or grossly perturbed[10]. The deleted elements are antennal or pre-antennal in their segmental origin (Fig. 1). Structures corresponding to the labral, intercalary and gnathal (mandibular, maxillary, and labial) segments develop, but are often disrupted, probably as a result of abnormal head involution. No evidence for homeotic transformation or duplication of head structures is found in *otd* embryos. Analysis of the cuticular phenotype of the head, which

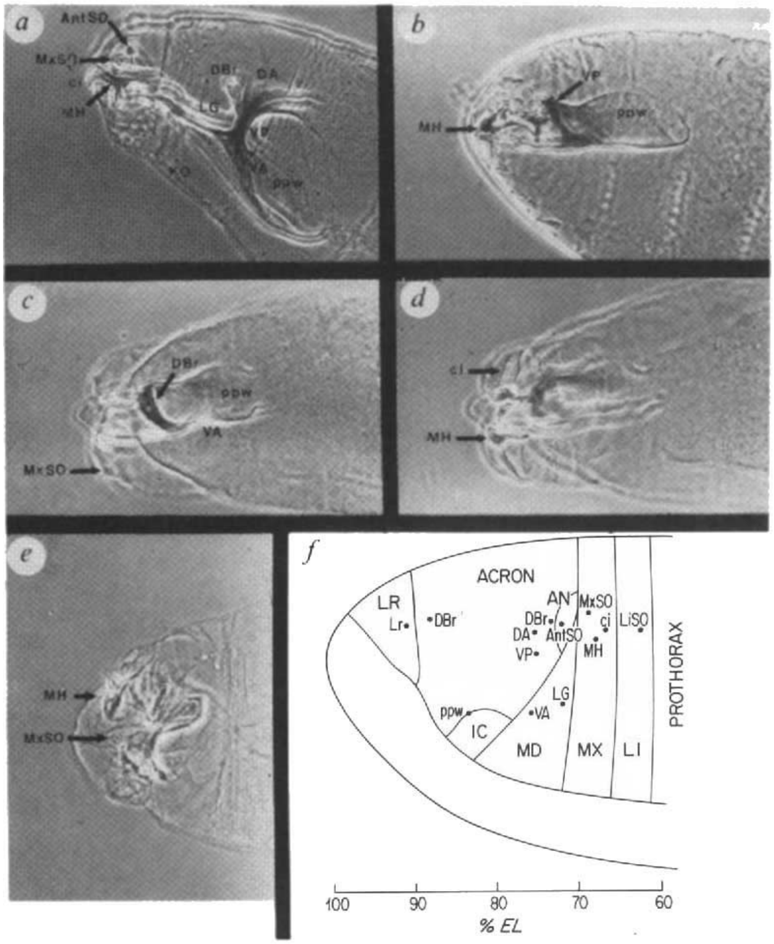

FIG. 1 Head defects in *otd* embryos. *a*–*e*, Phase contrast micrographs of cuticular preparations of wild-type (*a*) and *otd* mutant embryos (*b*–*e*). For abbreviations, see below. For a detailed description of wild-type head cuticular structures and sense organs, see ref. 24. Anterior is to the left in all panels. *b* and *c*, VA and ppw, which are of mandibular and intercalary origin respectively. The DBr and VP, additional elements of the cephalopharyngeal skeleton, are also present. The DA, which are derived from the pre-antennal region, are either absent or fragmented. *d*, Derivatives of the maxillary segment, the cirri and mouth hooks, are present in *otd* embryos. *e*, Absence of the AntSO and the presence of the MxSO; the LiSO is also present (not shown). The dorsal-medial papilla, which is probably pre-antennal in origin (S. Cohen and G. Jurgens, personal communication) is deleted (not shown). *f*, Fate map of the embryonic head at the blastoderm stage (adapted from Jurgens *et al.*[24]). Segmental assignment is based on the defects produced by laser irradiation at this stage of development. The labral, antennal, intercalary, mandibular, maxillary and labial segment boundaries are demarcated, and the fate map positions of several head structures indicated. Abbreviations: antennal sense organ, AntSO; antennal segment, AN; cirri, ci; dorsal arms, DA; dorsal bridge, DBr; egg length, EL; intercalary segment, IC; Keilin's organ, KO; labial sense organ, LiSO; labial segment, LI; labral segment, LR; labrum, lr; lateralgrate, LG; mandibular segment, MD; maxillary segment, MX; maxillary sense organ, MxSO; mouth hooks, MH; posterior wall of the pharynx, ppw; ventral arms, VA; vertical plate, VP.
METHODS. Cuticles were prepared as described previously[25]. The cuticular phenotypes shown are similar for two ethylmethane sulphonate-induced mutant alleles, otd^{XD87} and otd^{YH13}, and one deficiency allele, otd^{JA101} (refs 10, 30).

is difficult in first instar larvae, is supported by the expression patterns of the segment polarity genes *engrailed* (*en*) and *wingless* (*wg*) in the developing embryo (Fig. 2*a*, *c*). In addition to the reiterated stripes marking the gnathal, thoracic and abdominal segments, each of these genes is expressed in a specific, segmental pattern in more anterior head regions (refs 11–13; S. Cohen, personal communication). In *otd* mutant embryos, the expression of *en* and *wg* in antennal and pre-antennal regions is deleted (Fig. 2*b*, *d*). Consistent with the cuticular *otd* phenotype, expression corresponding to the labral, intercalary and gnathal segments is present in *otd* embryos.

To determine the relationship between the head phenotype observed in mutant embryos and *otd* expression, we analysed the early pattern of *otd* transcription (Fig. 3). Transcription is evident before cellularization at stage 4 of embryonic development and is restricted to a circumferential anterior region extending to the pole of the embryo. By the time cellularization is complete, *otd* expression has retracted from the pole and is confined to a broad circumferential stripe extending from 70 to 90% of the egg length, which subsequently diminishes in intensity ventrally. Expression is also detectable in the yolk nuclei within the region of the stripe (data not shown). The

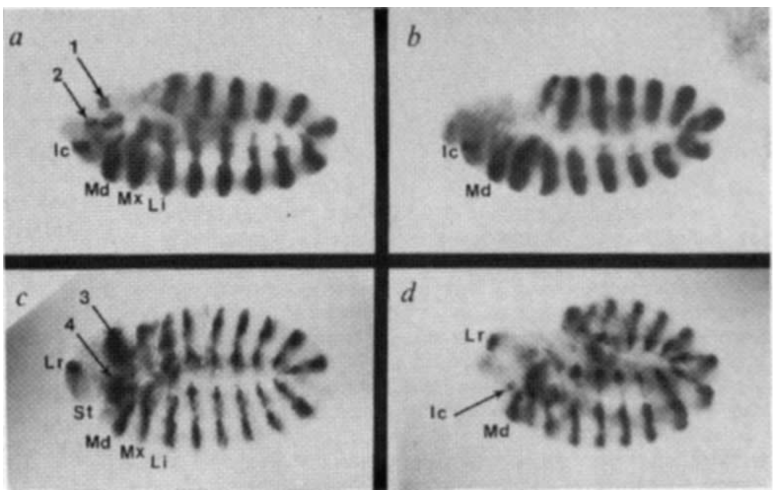

FIG. 2 Specific elements of *engrailed* (*en*) and *wingless* (*wg*) head expression are deleted in *otd* mutant embryos. *a* and *b*, Expression pattern of *en* at the germ band-extended stage in wild-type and *otd* embryos, respectively. In wild-type embryos, *en* is expressed anterior to the gnathal segments (Md, Mx and Li) in the intercalary (Ic) and antennal (arrow 2) segments (ref. 11; S. Cohen, personal communication). In addition, a pre-antennal spot of expression (arrow 1) is visible. In *otd* embryos, the antennal and pre-antennal regions of *en* expression are deleted, but expression in the intercalary and gnathal segments is retained. *c* and *d*, Expression pattern of *wg* in wild-type[12,13] and *otd* embryos, respectively. Expression in the stomodeal (St), labral (Lr), antennal (arrow 4) and pre-antennal (arrow 3) regions is visible. Expression in the intercalary segment is present, but cannot be seen in this focal plane. In an *otd* embryo (*d*), the deletion of the regions of antennal and pre-antennal staining can be seen. Expression of *wg* marking the Ic and Lr segments is retained. In all panels, anterior is to the left and dorsal at the top.
METHODS. Expression of *en* and *wg* were monitored using two *lacZ* insertion strains that accurately reproduce the embryonic patterns of protein expression of *en* (C. Hama and T. Kornberg, personal communication; ref. 26) and *wg* (N.P. and J. Kassis, unpublished observations). Females heterozygous for *otd* mutations were crossed with males from either *lacZ* strain. The *lacZ* expression was detected using an antibody to β-galactosidase with processing as previously described[26].

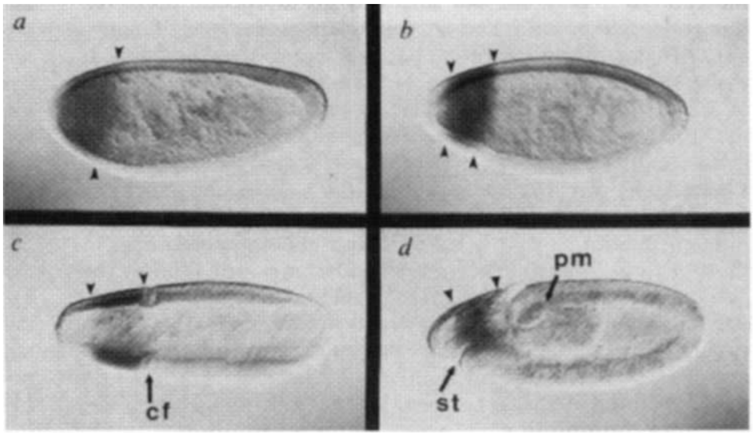

FIG. 3 Early expression of *otd* during embryogenesis. In all panels, anterior is to the left and dorsal at the top, except for *c* which is a dorsal view. Small arrows indicate the anterior–posterior boundaries of the domains of *otd* transcription. *a*, Expression of *otd* in a late stage-4 embryo; transcription can be seen in the anterior region. *b*, Cellularized stage-5 embryo; *otd* expression has retracted from the anterior pole, and forms a circumferential stripe extending from 70 to 90% egg length. Transcription diminishes in the ventral region of the stripe during subsequent stages. *c*, During early gastrulation in stage-6 embryos, the cephalic furrow forms just posterior to the domain of *otd* transcription. In germ band-extended embryos (stage 8), *otd* expression is localized to the procephalic head region. Staging of embryos was according to Campos-Ortega and Hartenstein[27]. Abbreviations: cephalic furrow, cf; stomodeum, st; posterior midgut, pm.
METHODS. *In situ* hybridization to whole-mount embryos was performed according to Tautz and Pfeifle[28]. The probe used for digoxygenin-labelling was a 3.8-kilobase *otd* complementary DNA (ref. 30).

formation of the cephalic furrow occurs just posterior to the domain of *otd* expression. By the extended germ-band stage, *otd* transcription is localized within the head region.

We have previously characterized the *otd* gene and shown that it encodes a predicted homeodomain protein[30]. Homeodomains can be classified according to the amino acid at position 9 of the putative recognition helix, which has been shown to confer binding specificity[14,15]. The *otd* and *bcd* gene products[16,17] are the only known proteins with a lysine residue at this position of the homeodomain.

The expression of *otd* is positively regulated by *bcd* in a concentration-dependent fashion (Fig. 4*a*–*g*). In embryos lacking maternal *bcd* product, *otd* transcription is absent. As the number of copies of *bcd* increases, the domain of *otd* transcription extends progressively towards the posterior end of the embryo. The expression of *otd* is negatively regulated by *tor*; in the absence of maternal *tor* activity, *otd* transcription fails to retract from the anterior 10% of the embryo (Fig. 4*c*). A similar effect has been observed for zygotic *hb* expression[9].

As the effect of *hb* mutations on head development[18] does not account for the absence of all head structures in *bcd* embryos the existence of an additional *bcd*-regulated gene(s) has been proposed[9]. Driever *et al.*[9] postulated the existence of a gene(s) which would be activated by higher *bcd* concentrations than is *hb* and specify all or part of the anterior head region. The predicted domain of expression of such a gene would therefore be localized within the anterior region of the *hb* domain of transcription. The *otd* gene, which is required for the development of structures from the antennal and pre-antennal head segments, fulfills these criteria. In addition to *otd*, the gene *empty spiracles* (*ems*)[19], which is also required for head development, is expressed in a circumferential stripe in the anterior region of

FIG. 4 Expression of *otd* is regulated positively by *bcd* and negatively by *tor*. *a*–*f*, *In situ* hybridization to embryos of various maternal genotypes. Anterior, left; all views are dorsal except *b*, which is lateral. *a*, *b*, *d*, *e* and *f*, Embryos derived from mothers carrying 0, 1, 2, 4, and 6 copies, respectively, of the wild-type *bcd* gene. The posterior extent of *otd* transcription is progressively extended as *bcd* dosage increases; *g* depicts this shift graphically. The *otd* points (●) indicate the position of the posterior limit of *otd* expression as a function of maternal *bcd* dosage. In all cases, measurements were made using dorsal views. In addition, the effect of maternal *bcd* dosage on *bcd* protein expression is shown. The *bcd* points (□) indicate the egg length position at which the same level of *bcd* protein is found for embryos derived from females with varying *bcd* dosages. The 65% value of *bcd* immunostaining intensity was chosen arbitrarily. Data is derived from ref. 29. *c*, Expression of *otd* in an embryo lacking maternal *tor* product; *otd* expression fails to retract from the anterior pole at the cellular blastoderm stage. Arrowheads in all panels show the anterior and posterior position of the domain of *otd* expression.
METHODS. *In situ* hybridization was as in Fig. 3. The genotypes of the females that produced embryos with 0, 1, 2, 4 and 6 copies of bcd^+ were respectively: bcd^{E1}/bcd^{E1}, $bcd^{E1}/\pm$, $\pm/\pm$, $BB9+BB16/\pm$ and $BB9+BB16/BB9+BB16$. The $BB9+BB16$ chromosome contains three copies of a wild-type *bcd* gene (G. Struhl, personal communication). The *tor* mutant embryos were derived from tor^{wk34}/tor^{wk34} homozygous females[1].

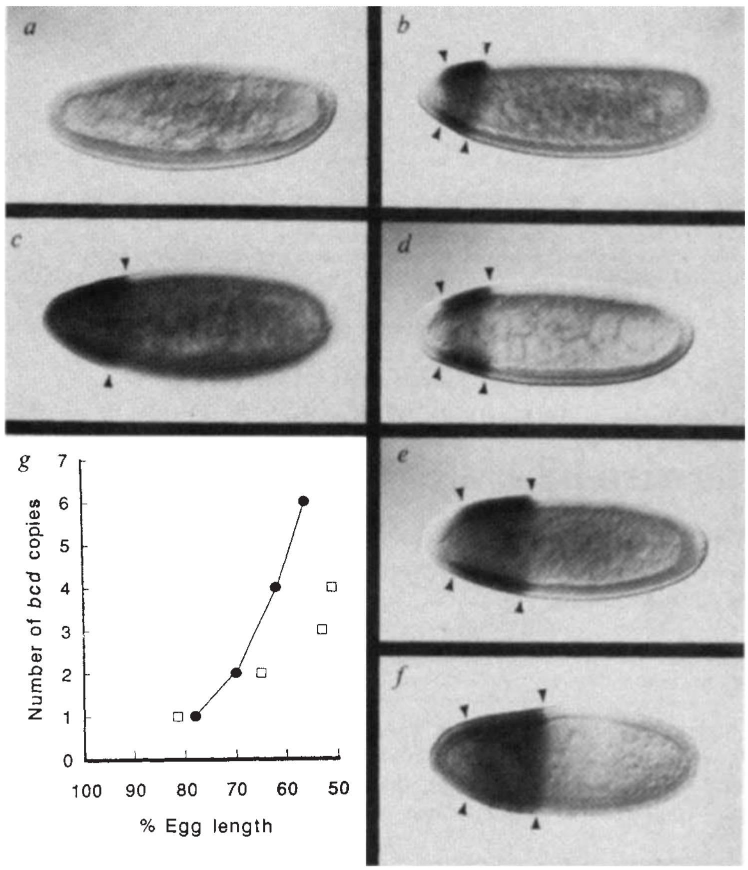

the embryo[20]. Both the *otd* and *ems* genes encode predicted homeodomain proteins and are dependent on the level of maternal *bcd* gene product for the establishment of their domains of expression. Mutations at each of these loci cause the deletion of subsets of adjacent head segments and show no evidence for the homeotic transformation of structural elements. If these genes are indeed directly transcriptionally activated by *bcd* (as suggested by the early appearance of their expression), then the regulation of *Drosophila* embryonic head development may be different from that of the thoracic and abdominal regions. In those regions, the earliest zygotic regulation is provided by the gap genes, several of which encode zinc-finger-containing proteins[21-23] required for the sequential activation of the downstream pair-rule and segment polarity genes. In the head, however, homeobox genes such as *otd* and *ems* may function as direct intermediaries between the *bcd* morphogen and the segment polarity genes. □

Received 20 April; accepted 25 May 1990.

1. Nusslein-Volhard, C., Frohnhofer, H. G. & Lehmann, R. *Science* **238**, 1675–1681 (1987).
2. Manseau, L. J. & Schupbach, T. *Trends Genet.* **5**, 400–405 (1989).
3. Frohnhofer, H. G. & Nusslein-Volhard, C. *Nature* **324**, 120–125 (1986).
4. Akam, M. *Development* **101**, 1–22 (1987).
5. Ingham, P. W. *Nature* **335**, 25–33 (1988).
6. Driever, W. & Nusslein-Volhard, C. *Cell* **54**, 83–93 (1988).
7. Driever, W. & Nusslein-Volhard, C. *Nature* **337**, 138–143 (1989).
8. Struhl, G., Struhl, K. & Macdonald, P. M. *Cell* **57**, 1259–1273 (1989).
9. Driever, W., Thoma, G. & Nusslein-Volhard, C. *Nature* **340**, 363–367 (1989).
10. Wieschaus, E., Nusslein-Volhard, C. & Jurgens, G. *Wilhelm Roux Arch. dev. Biol.* **193**, 286–307 (1984).
11. Dinardo, S., Kuner, J., Theis, J. & O'Farrell, P. *Cell* **43**, 59–69 (1985).
12. Baker, N. *Development* **103**, 289–298 (1988).
13. van den Heuvel, M., Nusse, R., Johnston, P. & Lawrence, P. *Cell* **59**, 739–749 (1989).
14. Hanes, S. D. & Brent, R. *Cell* **57**, 1275–1283 (1989).
15. Treisman, J., Gonczy, P., Vashishtha, M., Harris, E. & Desplan, C. *Cell* **59**, 553–562 (1989).
16. Frigerio, G., Burri, M., Bopp, D., Baumgartner, S. & Noll, M. *Cell* **47**, 735–746 (1986).
17. Berleth, T. *et al. EMBO J.* **7**, 1749–1756 (1988).
18. Lehmann, R. & Nussiein-Volhard, C. *Devl Biol.* **119**, 412–417 (1987).
19. Jurgens, G., Wieschaus, E., Nusslein-Volhard, C. & Kluding, H. *Wilhelm Roux Arch. dev. Biol.* **193**, 283–295 (1984).
20. Dalton, D., Chadwick, R. & McGinnis, W. *Genes Dev.* **3**, 1940–1956 (1989).
21. Rosenberg, U. B. *et al. Nature* **319**, 336–339 (1986).
22. Tautz, D. *et al. Nature* **327**, 383–389 (1987).
23. Nauber, U. *et al. Nature* **336**, 489–492 (1988).
24. Jurgens, G., Lehmann, R., Schardin, M. & Nusslein-Volhard, C. *Roux Arch. dev. Biol.* **195**, 359–377 (1986).
25. van der Meer, J. *Dros. Inf. Serv.* **52**, 160 (1977).
26. Klingensmith, J., Noll, E. & Perrimon, N. *Devl Biol.* **134**, 130–145 (1988).
27. Campos-Ortega, J. A. & Hartenstein, V. in *The Embryonic Development of* Drosophila melanogaster (Springer-Verlag, New York/Berlin, 1985).
28. Tautz, D. & Pfeifle, C. *Chromosoma* **98**, 81–85 (1989).
29. Driever, W. & Nusslein-Volhard, C. *Cell* **54**, 95–104 (1988).
30. Finkelstein, R., Smouse, D., Capaci, T. M., Spradling, A. C. & Perrimon, N. *Genes Dev.* (in the press).

ACKNOWLEDGEMENTS. We thank E. Wieschaus, G. Struhl, R. Lehmann, C. Hama and T. Kornberg for stocks, B. Noll for excellent technical assistance, S. Cohen and G. Jurgens for communication of unpublished results, and L. Spain, A. Brand, R. Binari, J. Klingensmith and E. Siegfried for critical reading of the manuscript. This work was supported by the Howard Hughes Medical Institute (N.P.) and the NIH (R.F.).

Detection and characterization of a folding intermediate in barnase by NMR

Mark Bycroft, Andreas Matouschek, James T. Kellis Jr, Luis Serrano & Alan R. Fersht*

MRC Unit for Protein Function and Design, Department of Chemistry, University of Cambridge, Lensfield Road, Cambridge CB2 1EW, UK

PROTEIN engineering is being developed for mapping the energetics and pathway of protein folding. From kinetic studies on wild-type and mutant proteins, the sequence and energetics of formation of tertiary interactions of side chains can be mapped and the formation of secondary structure inferred[1,2]. Here we cross-check and complement results from this approach by using a recently developed procedure that traps and characterizes secondary structure in intermediate states using ^{1}H NMR[3,4]. The refolding of barnase is shown to be a multiphasic process in which the secondary structure in α-helices and β-sheets and some turns is formed more rapidly than is the overall folding.

* To whom correspondence should be addressed.

It is desirable to corroborate the results of the novel procedure of detecting and characterizing an intermediate in the refolding of barnase by protein engineering methods[2], with a second technique. The method of choice is the NMR-hydrogen-exchange procedure of Udgaonkar and Baldwin[3] and Roder *et al.*[4] because it can detect individual interactions as well as gross structure. Their procedure is based on the observation that protons that are in NH···O=C hydrogen bonds are protected to varying extents against exchange with solvent[3,4]. Samples are taken from a reaction mixture in which a deuterated protein is being refolded in D_2O and NMR is used to examine which of the ND groups are in rapid exchange and which are protected. By this means, it was shown that the repeating secondary structure in regions of β-sheet in RNase A (ref. 3) and α-helices in cytochrome *c* (ref. 4) are formed faster than is the final folded structure.

The refolding of barnase was first monitored by the change in the fluorescence of its three tryptophan residues under identical conditions to those used in the NMR experiments (Fig. 1, 1.3 M (deuterated) urea, 99.8% D_2O, pD 6.3 at 25 °C). There is a fast phase accounting for 80% of the reaction, which has a half life of about 140 ms, and a slow phase of 20%, which is 50 times slower with a half life of 8.5 s. The latter phase corresponds to the interconversion from *cis* to *trans* of the fraction of proline residues that equilibrate in the unfolded enzyme—the native enzyme has three proline residues that are all *trans*[1,2]. There is some hint that the fast phase could be resolved into two phases of rate constant 11–16 s^{-1} and 4.6 s^{-1} (Fig. 1).

NMR experiments were made possible by assigning more than 99% of the proton resonances in the ^{1}H NMR spectrum of barnase to their amino-acid residues[5]. Some 45 of the backbone NH protons in the folded protein undergo slow exchange with solvent because they are involved in hydrogen bonds in secondary and tertiary structure. Barnase was denatured and all exchangeable NH groups deuterated (>90% exchange) by incubating in 6.5 M (deuterated) urea and 99.8% D_2O at pD 6.3. The denatured and deuterated protein was allowed to refold by diluting fivefold into D_2O at 25 °C. Samples were taken during the refolding process and exposed for 5–15 s to a labelling pulse of H_2O buffered at pH 8.5 where there is fast exchange of unprotected ND deuterons ($t_{1/2} \sim 5$ ms; refs 3, 4). The pH was lowered to 3.5, where exchange is very slow, and the fraction of H-exchange measured by two-dimensional (2-D) NMR.

It is found (Fig. 2) that 29 of the positions are sufficiently protected under the experimental conditions that the change in protection with time may be followed. Three of the positions, ND(H)s of Ile 25, Asn 77 and Ser 50, are protected according to a time course that is essentially identical to that of the overall refolding process (Fig. 3). Defining the fraction of protons in rapid exchange at zero time as 1.0, compared with 0 when protected in the fully folded protein, the amplitude of the kinetic changes is 0.74–0.76. The theoretical maximum amplitude for the fast phase is 0.8, as 20% of the protein folds slowly, limited by the proline isomerization. Significantly, Ile 25, Asn 77 and Ser 50 make tertiary hydrogen bonds that are not within regular secondary structure but are a consequence of the overall fold of the molecule. It is found, however, that several of the deuterons in the regular secondary structure become protected much faster (Fig. 3 and Table 1). The time courses for many of these are at least biphasic, the slower phase varying from 10–28 s^{-1}, with an amplitude of 50–80% of the maximum. The fastest phase(s) is generally complete by 5 ms and has a smaller amplitude of 10–50%. Multiphasic exponential curves are notoriously